UMT PRESS

Journal of Sustainability Science and Management
Journal Homepage: https://jssm.umt.edu.my
eISSN: 2672-7226
DOI: http://doi.org/10.46754/jssm.2026.04.003

FUTURE CHANGES OF PHYSICAL-BIOGEOCHEMISTRY (1990–2060) IN THE SOUTH CHINA SEA UNDER RCP8.5 CLIMATE CHANGE SCENARIO

ALLIA AFIQAH[1]*, NUR HIDAYAH ROSELI[1,2], WINFRED MARSHAL[2], MOHD FADZIL MOHD AKHIR[2], ROSWATI MD. AMIN[1], ANNA KATAVOUTA[3] AND JEFF POLTON[3]

[1]Faculty of Science and Marine Environment, Universiti Malaysia Terengganu, 21030 Kuala Nerus, Terengganu, Malaysia.
[2]Institute of Oceanography and Environment, Universiti Malaysia Terengganu, 21030 Kuala Nerus, Terengganu, Malaysia.
[3]National Oceanographic Centre, Joseph Proudman Building, 6 Brownlow Street, Liverpool L3 5DA, United Kingdom.

**Corresponding author: p5913@pps.umt.edu.my*

ARTICLE INFO

Article History:
Received:12 September 2024
Revised: 21 October 2025
Accepted: 28 October 2025
Published: 15 April 2026

Keywords:
Climate change, biogeochemistry, ocean warming, productivity, projection model.

ABSTRACT

The South China Sea (SCS), one of the world's most productive and commercially valuable fishing grounds and vital coral reef systems is particularly vulnerable to climate-induced ocean changes. Rising temperatures, ocean acidification, shifts in salinity, and other environmental factors driven by climate change pose uncertain but potentially profound risks to human and natural systems in the region. This study focused on three upwelling zones in SCS, located between 100 ºE – 119 ºE and 0 ºN – 13 ºN, western SCS (Vietnam), southern SCS on the east coast of Peninsular Malaysia (ECPM), and eastern SCS (Sabah). Using a coupled physical-biogeochemical model at ~ 7 km resolution under the RCP8.5 scenario, this study projects marine environmental changes from 1990 to 2060 to assess the impacts of climate change on nutrient dynamics and overall ocean health. Eight surface physical–biogeochemical parameters: SST, SSS, diatom, NO_3, NH_4, O_2, microphytoplankton, and microzooplankton were observed across monsoonal (SWM & NEM) and decadal trends (1990 – 2060). The SCS recorded a regional SST increase of ~1.3°C and a salinity drop of over 0.3 psu throughout the study period. Biogeochemical parameters also showed declining trends, indicating potential shifts in primary productivity. Surface O_2 concentrations significantly decreased (-10 mmol O_2/m^3), suggesting broader implications for ocean health. These biogeochemical declines were most pronounced in the western, eastern, and southern SCS, largely driven by rising SST and changes in wind patterns. This study highlights a significant warming of up to 5.2%, salinity decline exceeding -1.5%, and widespread reductions in phytoplankton and zooplankton biomass reaching -19.9% by mid-century. These environmental shifts are likely to impact marine biodiversity, disrupt small-scale fisheries, and pose risks to food security across the region. This study provides valuable insights into the changes of physical and biogeochemistry trends under climate change, supporting future adaptation strategies for ecosystem management and coastal resilience.

Introduction

The South China Sea (SCS) is a vital region because it has economic, ecological, and climatic importance. Since it's the largest in Southeast Asia as a semi-closed marginal sea, encompasses an impressive variety of ecosystems and serves as the habitat for a diverse range of marine creatures. The SCS is among the most climate-sensitive continental shelf regions with regard to changes in temperature, sea levels, and biogeochemical cycles. Several countries such as Malaysia, Vietnam, Thailand, Philippines, China, Taiwan, and Hong Kong are part of this region. Located in Southeast Asia, the SCS is the largest marginal sea in that the region and it has a significant impact on regional and global climates (Hu *et al*., 2000). The bathymetry of the SCS features the Sunda Shelf, a shallow continental shelf in the southern region with an average depth of less than 100 m, connected to a deeper continental slope and central basin (Roseli *et al*., 2022).

The SCS exhibits seasonal variability driven by (Tan *et al*., 2006), two distinct monsoon seasons: The Northeast Monsoon (NEM) and the Southwest Monsoon (SWM). The NEM, which occurs from between December and February (DJF), brings cool, wet winds from the Asian continent, leading to lower sea temperatures. In contrast, the SWM, which occurs from between June and August (JJA), brings warm, dry winds from the Indian Ocean, leading to higher sea temperatures. Transitional periods between these monsoons typically occur in April and October (Thia-Eng *et al*., 2000; Roseli & Akhir, 2014). The NEM brings higher annual rainfall to Southeast Asia than the SWM (Hastenrath, 2015). Additionally, the SCS is affected by inter-annual and decadal sea-level changes linked to El Nino Southern Oscillation (ENSO) and the Pacific Decadal Oscillation (PDO) in Pacific Ocean, as well as the Indian Ocean Dipole (IOD) in the Indian Ocean (Soumya *et al*., 2015).

The world's oceans are getting warmer, more acidic, and losing oxygen, causing marine species to shift their geographical ranges. It is estimated that the changes will accelerate in this century (IPCC, 2019). The SCS is particularly vulnerable to the impacts of marine climate change due to its dense coastal population (Neumann *et al*., 2015) and heavy reliance on marine resources (Barange *et al*., 2014). Climate change is expected to affect marine fisheries through changes in ocean conditions, including rising sea temperatures, shifting currents, and altered coastal upwelling patterns (Brander, 2010; Sumaila *et al*., 2011; Weatherdon *et al*., 2016; Lam *et al*., 2020).

Modelling studies suggest a potential decline in fish production and associated revenue in the region under future climate scenarios (Stobutzki *et al*., 2006; Barange *et al*., 2014; Teh *et al*., 2019). Additionally, climate change is linked to increasing typhoon intensity and more frequent flooding events in the SCS, although considerable uncertainty remains regarding historical patterns and future projections (Lee *et al*., 2012; Ying *et al*., 2012; Loo *et al*., 2015; Knutson *et al*., 2020).

Ongoing climate change is expected to affect ocean biogeochemistry in multiple ways. Rising sea temperatures are projected to strengthen ocean stratification, which can reduce vertical nutrient transport and limit the availability of nutrients for surface-dwelling phytoplankton, ultimately decreasing primary productivity (Steinacher *et al*., 2010). These changes may also contribute to shifts in the distribution and abundance of marine species, including commercially important fish populations, as they respond to changing habitat conditions (Pinsky *et al*., 2013).

To better understand and project these complex changes, climate scenarios such as the Representative Concentration Pathways (RCPs) are used. These scenarios predict the future greenhouse gas concentrations based on socio-economic assumptions. The four RCPs range from very high (RCP8.5) through to very low (RCP2.6) future concentrations. The numerical values of the RCPs (2.6, 4.5, 6.0, and 8.5) refer to the concentration in 2100 (van Vuuren *et al*., 2011) and were adopted in the Fifth Assessment Report on Climate Change (IPCC) in 2014 as a basis for the report's findings.

RCP8.5, a high-emission "business-as-usual" scenario was selected for this study, which envisioned continued fossil fuel use, limited climate change policy implementation, and rapid growth (IPCC, 2014). It provides a strong basis for assessing worst-case climate impacts in the SCS, a region of high productivity and complex hydrography. RCP8.5 is widely used to stress-test marine ecosystems (Jacobs *et al*., 2021) and remains closely aligned with historical emission and mid-century projections under current policies (Schwalm *et al*., 2020). While lower-emission scenarios support mitigation planning, RCP8.4 helps evaluate maximum risk for marine adaptation strategies.

The influence of climate change on physical and biogeochemical conditions in Southeast Asia is a crucial consideration for addressing climate action and supporting life below the water as outlined in the United Nations (UN) Sustainable Development Goals 13 and 14. Although global climate models offer a broad perspective on environmental change (IPCC, 2019), their coarse and temporal resolution limits their ability to capture the ecological, social, and economic impacts of climate change on regional seas.

Although the central and northern regions of the SCS have been widely studied for their physical and biogeochemical variability (Cai *et al*., 2009; Ning *et al*., 2009; Ma *et al*., 2013), the three major upwelling zones remain comparatively understudied. This research addresses that gap by examining long-term changes in physical and biogeochemical conditions under a climate change scenario across these key upwelling regions in the SCS. It is hypothesised that regional warming, combined with spatial variations in biogeochemical cycling and weakening seasonal wind stress over upwelling zones may drive a sharper decline in nutrient levels and productivity (Marshal *et al*., 2025).

Materials and Methods

Model Description and Setup

In this study, researchers used simulated outputs from a three-dimensional modelling framework that coupled an ocean circulation model with a marine biogeochemistry and lower trophic level ecosystem model (Figure 1).

The ocean circulation model known as the Nucleus for European Modelling of the Ocean (NEMO) is a physical ocean circulation model designed for both regional and global configurations. NEMO outputs simulate three-dimensional fields of velocity, sea surface height, temperature, and salinity. These outputs drive the coupled biogeochemical model by influencing biological rates and transporting biogeochemical tracers (Buttenschon *et al*., 2016).

The biogeochemical and ecological model European Regional Seas Ecosystem Model (ERSEM) is a comprehensive framework that simulates both pelagic and benthic environments. It represents key biogeochemical cycles, including carbon, nitrogen, phosphorus, silicate, iron, and oxygen, it incorporates multiple functional types of phytoplankton, zooplankton, and benthic fauna. ERSEM also includes a detailed microbial loop and the marine carbonate system (Buttenschon *et al*., 2016).

The model outputs used in this study are derived from a coupled physical-biogeochemical called NEMO-ERSEM simulation configured over the Southeast Asian regional shelf seas, including the SCS. The model has a horizontal resolution of ~ 7 km with 43 vertical layers, covering the period between 1990 and 2060 at both monthly and daily intervals. The outputs are provided in NetCDF (.nc) format and adhere to the Climate and Forecast (CF) Metadata Convention version 1.7 and the Attributed Convention for Dataset Discovery (ACDD) version 1.3. Indicators from NEMO-ERSEM are provided on the basis of the Intergovernmental Panel on Climate Change (IPCC) Fifth Assessment Report scenarios with two RCPS, RCP8.5, and RCP4.5, but only the RCP8.5 scenario was used in this study.

The NEMO-ERSEM models were driven by projections from global climate models developed under the Coupled Model Intercomparison Project Phase 5 (CMIP5). These global outputs were interpolated onto the regional grid and used as open boundary conditions for both physical and biogeochemical components. Initial conditions for physical variables were sourced from the global models while biogeochemical variables were initialised using a combination of global datasets and hindcast simulations.

Figure 1 provides an overview of the coupled hydrodynamic-biogeochemical modelling framework. Among the four RCP of atmospheric CO_2 over the 21st century (van Vuuren *et al*., 2011), the high emission RCP8.5 scenario was used to force the Hadley Centre Global Environment Model version 2 (HadGEM2) Earth System Model (Figure 1; left). The HadGEM2-ES supplied atmospheric forcing, land-based runoff, and lateral boundary conditions for the regional model domain (Figure 1; middle). These inputs were used to drive the regional coupled system (Figure 1; right), which integrates the NEMO ocean circulation model (Figure 1; top right) coupled with the ERSEM ecological-biogeochemical model (bottom-right) (Clark & Lessin, 2019).

Atmospheric Forcing and Boundary Conditions

The model was forced using atmospheric inputs and open boundary conditions from the HadGEM2-ES global simulation under the RCP8.5 greenhouse gas emission scenario. (Hadley Centre Global Environment Model version 2 (HadGEM2) is fully coupled Earth System Model that integrates atmospheric and ocean systems, along with terrestrial vegetation, ocean biogeochemistry, and atmospheric chemistry (Collins *et al*., 2011; Clark & Lessin, 2019). HadGEM2-ES is well-suited as a forcing field due to its high performance in simulating large-scale climate patterns, particularly in the tropics and Asia-Pacific region. Developed under CMIP5, it provides comprehensive atmospheric, oceanic, and land-surface outputs.

Data Analysis

The coupled model was integrated from 1990 to 2060, producing a three-dimensional field of both physical and biogeochemical variables. In this study, eight key surface physical-biogeochemical parameters were selected to assess marine ecosystem health and productivity levels, based on established relevance on global and regional-scale studies (Bopp *et al*., 2013). Diatom nitrogen, along with microphytoplankton and microzooplankton biomass were included to evaluate food web responses. Oxygen (O_2) was selected to assess potential deoxygenation while nitrate (NO_3) and ammonium (NH_4) were chosen for their roles as essential nutrients influencing

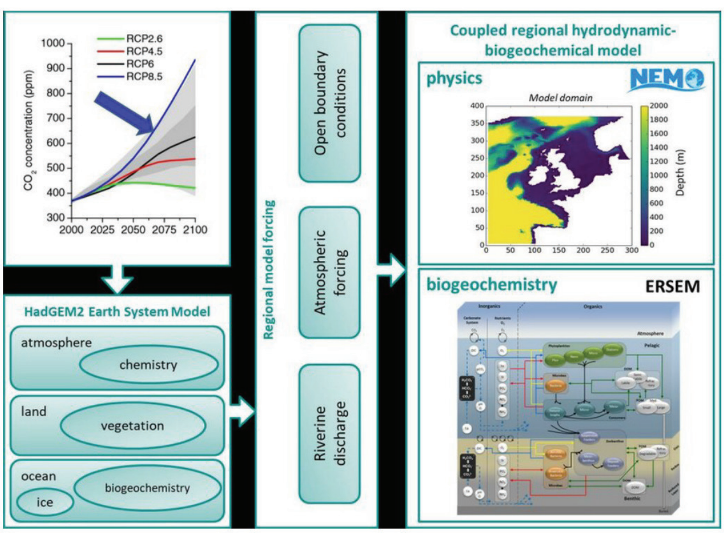

Figure 1: Overview of the coupled NEMO hydrodynamic and ERSEM biogeochemical model structure, driven by HadGEM2 Earth System Model outputs under the RCP8.5 greenhouse gas emission scenario. Figure adapted from Clark and Lessin (2019)

ecosystem dynamics under climate change. Sea Surface Temperature (SST) and Sea Surface Salinity (SSS) were also included to examine how physical changes influence biogeochemical processes. Collectively, these variables offer a comprehensive understanding of marine biogeochemical variability in the study region. In this phase, daily data from model outputs were first averaged seasonally into SWM, represented by June, July, and August (JJA) and NEM, represented by December, January, and February (DJF) for 70 years. The 70-year seasonal dataset was then averaged by decade for plotting purposes. Trend analysis was performed on the 70-year decadal dataset to assess interdecadal variation in future changes in physical-biogeochemistry parameters through different monsoon seasons.

Following this, the analysis integrated three components: Spatial mean climatology maps, interdecadal time series trends (between 1990 and 2060), and percentage change calculations, time series plots were used to reveal interdecadal variability and potential long-term shifts while percent changes highlighted the magnitude of projected anomalies across the SCS. Anomalies were calculated by subtracting the long-term baseline average (1990 – 1999) from the projected decadal mean values (e.g., between 2050 and 2060) for each physical and biogeochemical parameter.

Model Validation

To further ensure the reliability of trend results from the coupled physical-biogeochemical model, a quantitative assessment was performed. The performance of the coupled NEMO-ERSEM model was assessed using observational satellite data from the MODIS-Aqua SST Level-3 monthly product. Validation was conducted for two monsoon seasons, the SWM–JJA and the NEM–DJF across two decades (2000–2009 and 2010–2019). Modelled SST data from NEMO-ERSEM were spatially collocated and temporally averaged to match MODIS-Aqua SST at 4-km resolution over the SCS domain (100°E–119°E; 0°N–13°N).

10 representative surface points were selected within the model domain, corresponding SST values from NEMO-ERSEM (~7 km resolution) and MODIS-Aqua (4 km resolution) were extracted at matching geographic coordinates. Statistical performance was assessed using the Root Mean Square Error (RMSE), Mean Bias Error (MBE), and coefficient of determination (R^2) to quantify the agreement between simulated and observed SST, as summarised in Table 1 and further illustrated in Figure 2, which depicts consistent temporal patterns across both datasets during JJA and DJF the periods between 2000 and 2009 as well as that of between 2010 and 2019.

Table 1: Statistical validation of NEMO-ERSEM model SST against MODIS-Aqua SST during JJA (SWM) and DJF (NEM) for two decades (2000–2009 and 2010–2019). The validation metrics (RMSE, MBE, and R^2) indicate high model skill and minimal bias

Monsoon Season	**Decade**	**RMSE**	**R^2** (°C)	**MBE**
JJA (SWM)	2000–2009	0.1875	0.992	0.1293
DJF (NEM)	2000–2009	0.2711	0.9581	0.0911
JJA (SWM)	2010–2019	0.5627	0.8554	0.161
DJF (NEM)	2010–2019	0.3107	0.9624	0.1214

Comparison of NEMO-ERSEM model and MODIS-Aqua observed SST during for 2000–2009 and 2010–2019	Comparison of NEMO-ERSEM model and MODIS-Aqua observed SST during DJF for 2000–2009 and 2010–2019

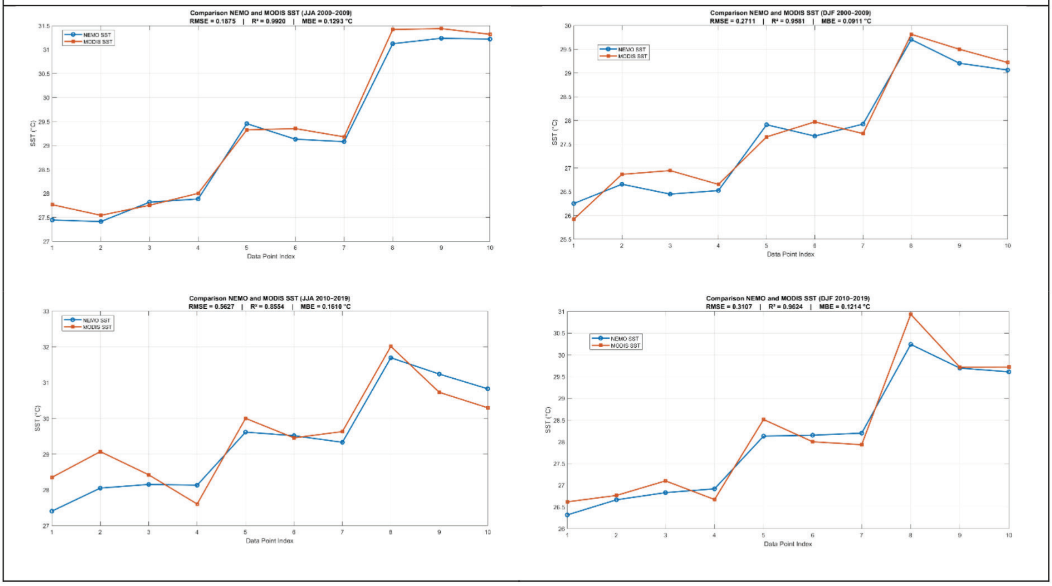

Figure 2: Comparison of NEMO-ERSEM modelled and MODIS-Aqua observed SST during JJA and DJF for 2000–2009 and 2010–2019. The model shows high consistency with observations, reflected by low RMSE and high R^2 values

As Sea Surface Temperature (SST) represents a primary physical driver in coupled physical–biogeochemical systems, its validation ensures the reliability of the model's thermal structure and surface forcing, which underpin all simulated biogeochemical processes. Due to limited satellite and in-situ coverage of biogeochemical variables in the SCS, the SST was selected as the principal parameter for model performance evaluation.

The validation results show a strong agreement between the NEMO-ERSEM model and MODIS-Aqua SST observations across all periods and monsoon seasons. High coefficients of determination (R^2 = 0.86–0.99) indicate that the model effectively reproduces observed SST variability. RMSE values ranging between 0.19°C and 0.56°C reflect low temperature deviations, confirming good model accuracy. The small positive MBE values (0.09°C–0.16°C) suggest a slight warm bias, particularly over the JJA period between 2010 and 2019, which may be associated with enhanced surface heating under stronger monsoonal forcing. Overall, these results demonstrate that the coupled NEMO-ERSEM model reliably captures the spatial and temporal SST patterns in the SCS, providing confidence in its use for analysing future physical–biogeochemical changes.

Study Area

Three upwelling zones in the SCS were selected for analysis (Figure 3): Box 1 (10 – 13 ºN, 108 – 112 ºE) represents the western SCS near Vietnam, Box 2 (3 – 6 ºN, 105 - 107 ºE) covers the southern SCS near ECPM, and Box 3 (3 – 6 ºN, 114 – 116 ºE) corresponds to the eastern SCS off Sabah. These regions were chosen to capture spatial variability across distinct upwelling in the SCS.

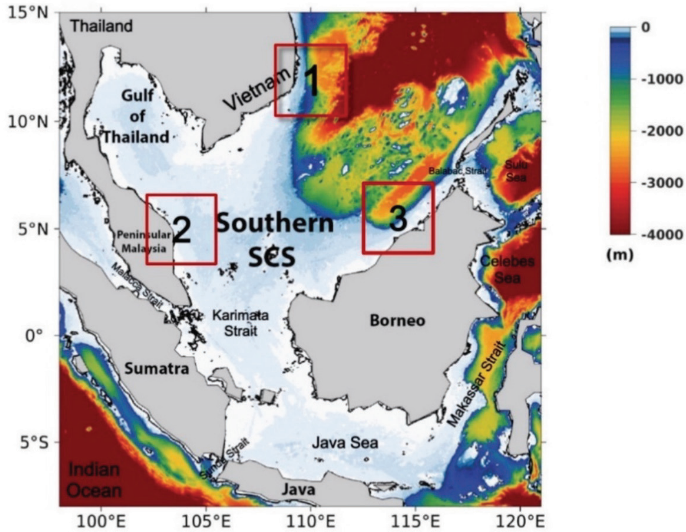

Figure 3: Map showing the bathymetry features of the study area. The red box indicates the region of interest for the interdecadal variability, highlighting three upwelling zones: 1 – western SCS (Vietnam), 2 – southern SCS (ECPM), and 3 – eastern SCS (Sabah)

Results and Discussion

Mean Climatology and Seasonal Variation

Presenting mean climatology helps identify consistent seasonal patterns and provide a baseline to assess long-term oceanographic and biogeochemical conditions. It averages data over decades to highlight typical seasonal trends while minimising short-term variability (Deser *et al*., 2010). In SCS, where monsoon systems strongly influence physical and biological processes, climatological analysis is crucial for comparing seasonal differences in temperature, salinity, nutrients, and productivity (Liu *et al*., 2002; Zhu *et al*., 2019).

Figure 4 demonstrated the seasonal mean climatology of eight surface physical-biogeochemistry parameters during the SWM and NEM. SST during SWM was notably higher, ranging between 28°C and 32°C while cooler temperatures were observed during NEM, ranging between 27°C and 30°C. These seasonal variations are consistent with Yang *et al*. (2013), who demonstrated that monsoonal wind patterns significantly influence surface heat fluxes in SCS. SSS exhibited distinct spatial patterns, with elevated salinity values (32 – 33.6 psu) in the western SCS during SWM and lower salinity (30 – 32.8 psu) observed during NEM, particularly along southern coast (Figure 4). During dry and warm SWM seasons, with less rain, the sea surface becomes warmer and saltier in comparison to other seasons (Siang *et al*., 2021).

Biogeochemical conditions in SCS vary clearly between the SWM and the NEM. During SWM, strong upwelling and mixing bring more nutrients to the surface, resulting in higher levels of diatom nitrogen (up to 0.5 mmol N/m^3) observed in the western and southern areas of the SCS, NO_3 (up to 3 mmol N/m^3), particularly along the coast of upwelling regions and Gulf of Thailand (GoT) and NH_4 (up to 0.5 mmol N/m^3), especially near the coast (Figure 4).

Surface O_2 is also higher over the SWM (200-250 mmol O_2/m^3) due to stronger mixing and higher phytoplankton activity (Ning *et al*., 2004), while NEM shows slightly lower O_2 level. In contrast, nutrient levels are lower during the NEM due to weaker mixing (Lu *et al*.,

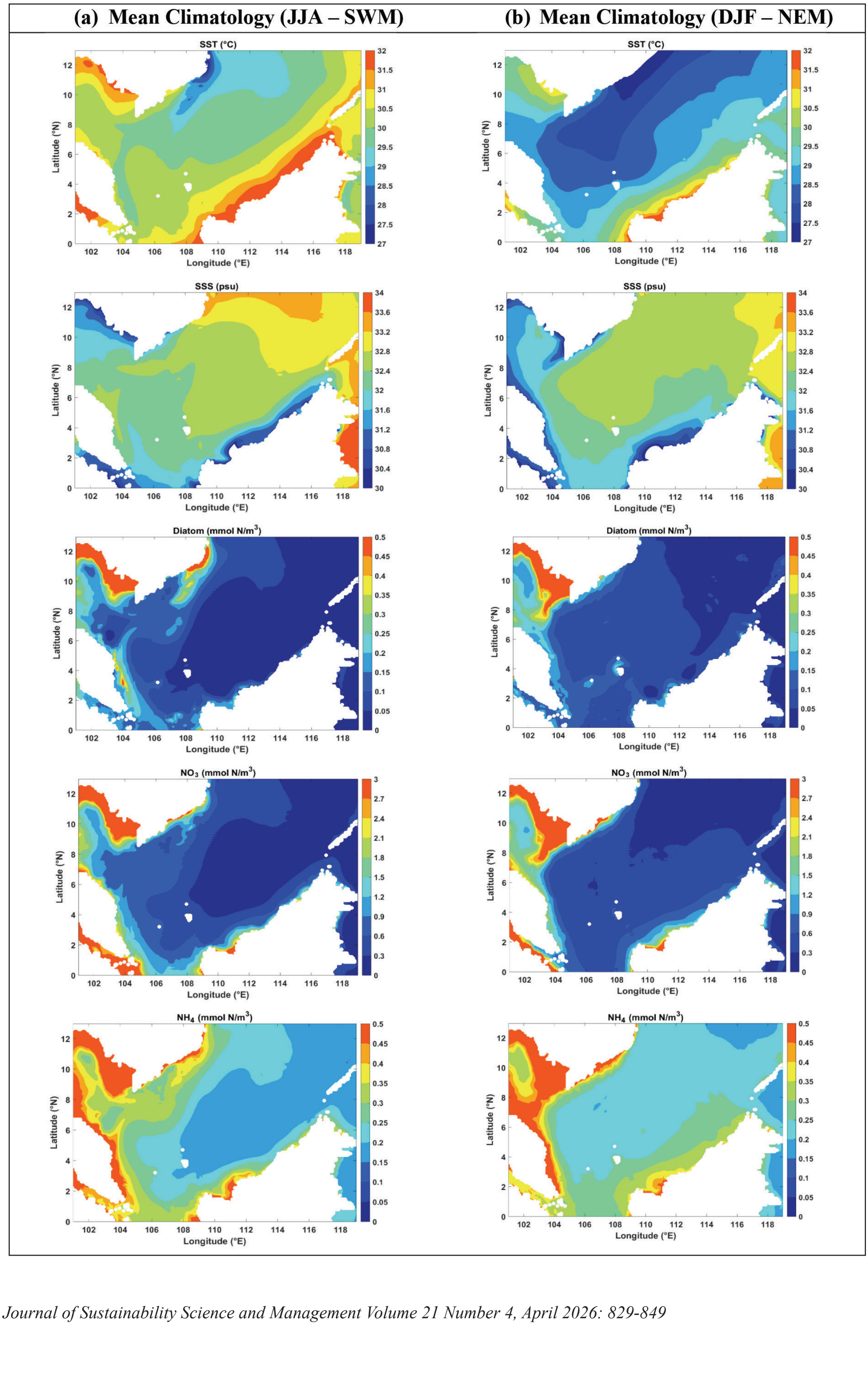
(a) Mean Climatology (JJA – SWM)
(b) Mean Climatology (DJF – NEM)
SST (°C)
SSS (psu)
Diatom (mmol N/m3)
NO3 (mmol N/m3)
NH4 (mmol N/m3)
Latitude (°N)
Longitude (°E)

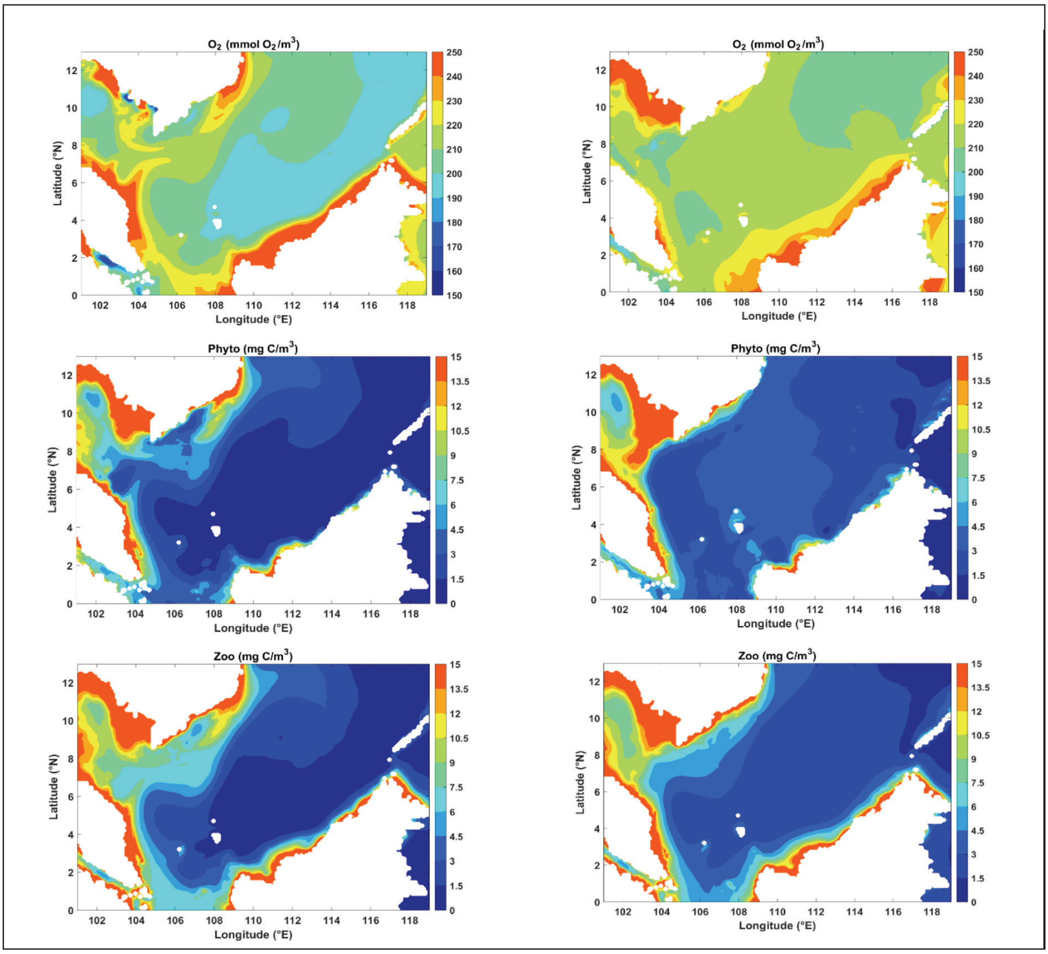

Figure 4: Mean climatology of eight surface physical-biogeochemical parameters including: SST, SSS, diatom nitrogen, NO_3, NH_4, O_2, microphytoplankton, and microzooplankton from 1990 to 2060 – (a) JJA (SWM) and (b) DJF (NEM)

2020; Tao *et al*., 2025). Microphytoplankton and microzooplankton also increase during SWM (up to 15 mg C/m^3) (Figure 4) due to better nutrient supply and higher productivity. These values drop during the NEM, reflecting lower biological activity (Liu *et al*., 2002; Calbet & Saiz, 2005).

Interdecadal Variability

To evaluate the impact of climate change, this study analysed monsoonal variability and long-term decadal trends in surface anomalies of physical and biogeochemical parameters using time series plots across three upwelling regions in the SCS, as shown in Figure 5. The observed fluctuations within the study area are likely influenced by climate variability under RCP8.5 scenario conditions. The SST anomalies show strong warming, reaching +1.3°C throughout both seasons, likely due to reduced convective cooling and intensified surface heat flux under RCP8.5 (Fang & Wu, 2008; Zhu *et al*., 2024).

Notable SST anomalies peaks correspond to major El Niño and IOD events. Marshall *et al*. (2025) reported that strong El Niño events occurred in 1997/1998, 2009/2010, and

2015/2016, while La Niña events followed in 1998/1999, 2010/2011, and 2016/2017. Positive IOD phases were recorded in 1997, 2009, and 2015, with negative IODs in 1998, 2010, and 2016. During these periods, the southern SCS experienced notable increases in SST, underscoring the combined impact of ENSO and IOD on surface conditions. Meanwhile, SSS shows declines (down to -0.3 psu) during both seasons observed in three upwelling zones in SCS (Figure 5). These decreasing trends suggest enhanced freshwater input and reduced surface salinity driven by intensified precipitation, linked to monsoon intensification and anthropogenic hydrological cycles under a global warming scenario (Chou *et al*., 2013).

Oxygen levels decline significantly during the SWM and the NEM to -10 mmol O_2/m^3, especially in eastern SCS, linked to stratification and reduced ventilation (Breitburg *et al*., 2018). Both NH_4 (-0.04 to 0.02 mmol N/m^3) especially in western SCS and NO_3 (-0.023 to 0.23 mmol N/m^3) particularly in eastern SCS increase across seasons, suggesting enhanced remineralisation and nutrient supply (Fu *et al*., 2012). Diatom nitrogen drops in SWM (-0.04 mmol N/m^3), particularly in the southern area of the SCS, indicating nutrient limitation (Roxy *et al*., 2015) but moderate changes throughout the NEM while microphytoplankton declined throughout the SWM (from +1.5 to -2.0 mg C/m^3), but slightly increased throughout the NEM (up to +1.8 mg C/m^3). Microzooplankton consistently decreased across both seasons (from +1.8 to -1.5 mg C/m^3) (Figure 5), which is indicative of disrupted trophic interactions and reduced grazing efficiency as primary production shifts under warming conditions. These trends align with projections of altered monsoon-driven nutrient dynamics in SCS under climate change, potentially reshaping phytoplankton community composition and productivity (Chen *et al*., 2023; Zhang *et al*., 2023).

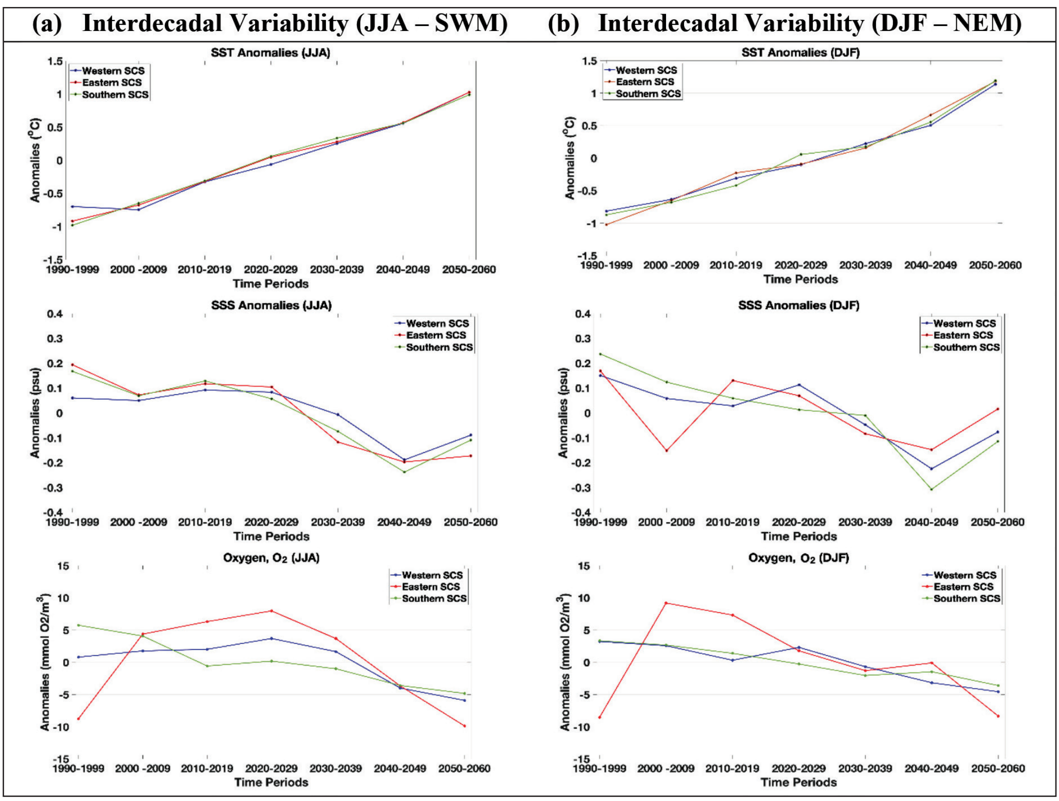

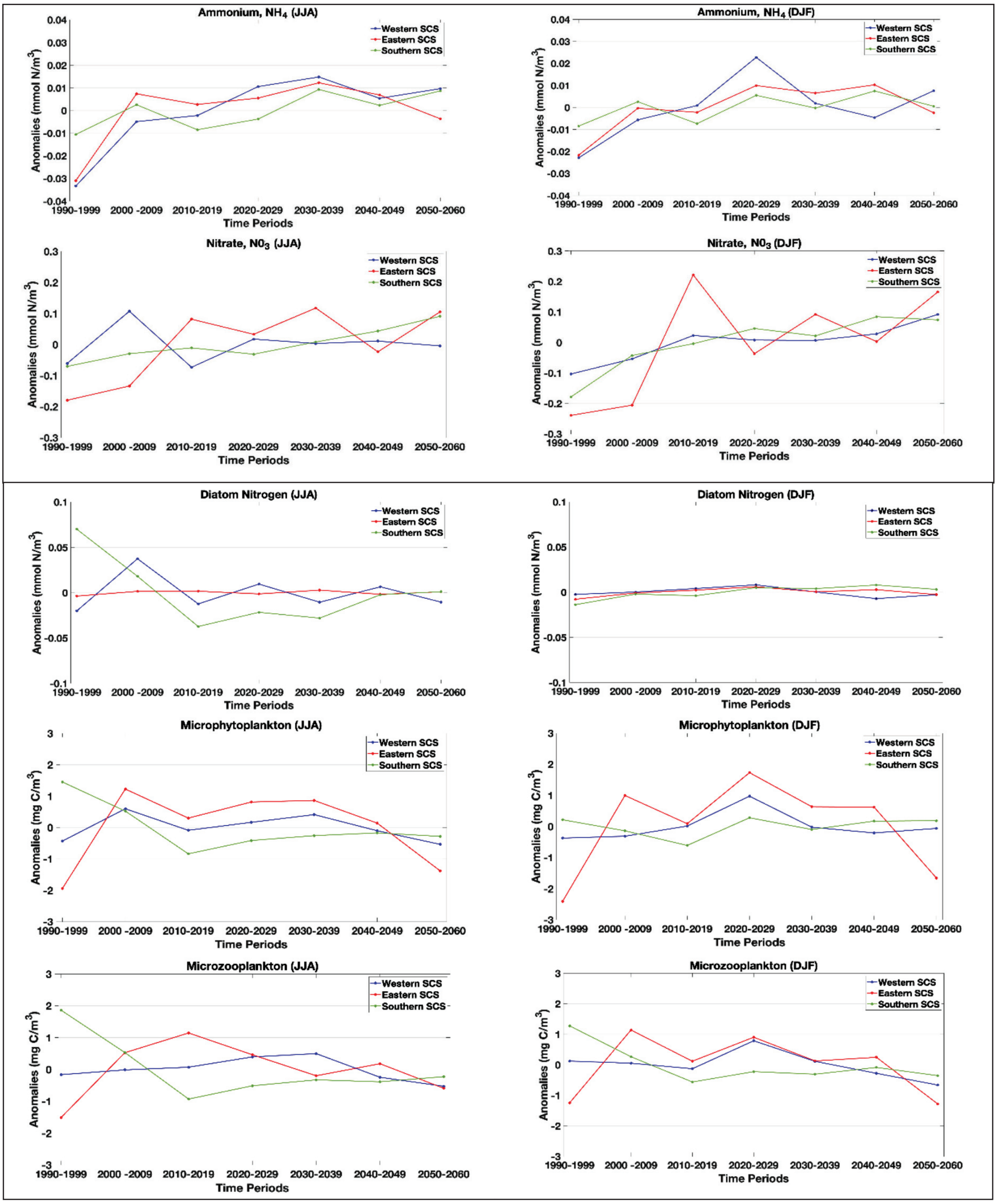

Figure 5: Interdecadal variability of surface physical-biogeochemistry parameters during (a) JJA (SWM) and (b) DJF (NEM). The blue line represents western SCS, red line represents eastern SCS, and green line represents southern SCS

According to Marshal *et al*. (2025), the study suggests that interannual biogeochemical variability is primarily driven by ENSO events while SST anomalies are influenced by the combined effects of ENSO and IOD. These climate drivers modulate upwelling intensity, nutrient availability, and thermal structure, ultimately shaping ecosystem responses and productivity patterns in the region. The ENSO plays a key role in influencing and upwelling and nutrient dynamics such as NO_3, thereby affecting the productivity patterns (Kok *et al*., 2019). The IOD can amplify or modify ENSO effects, leading to complex SST anomalies and shifts in monsoonal winds and rainfall patterns (Luo *et al*., 2010; Cai *et al*., 2012; Nur'utami & Hidayat, 2016; Zhang *et al*., 2019). The interplay between ENSO and IOD significantly shapes physical and biogeochemical variability, as reflected by the aligned peaks and throughs in observed anomalies (Marshal *et al*., 2025).

Changes of Physical-biogeochemical Parameters

The rest of this section discusses the mean changes of eight surface physical-biogeochemistry parameters over the 70-year period. It is a valuable metric for assessing long-term ecosystem responses to climate change, as it allows for direct comparison across regions and variables (Laufkotter *et al*., 2015; Kwiatkowski *et al*., 2020). The projected changes in SST between 1990 and 2060 indicate a consistent warming trend across SCS, with stronger increases over the DJF period (3.7% – 5.2%) as compared to over the JJA period (2.8% – 5.2%). Peak warming during DJF is observed in the central basin (110 °E) while JJA shows maximum increases in northern SCS (> 10° N) (Figure 6).

Coastal areas near Sabah coast exhibit relatively lower SST increases during JJA, likely due to seasonal upwelling. Similar spatial SST patterns have been reported in previous studies, where upwelling regions such as the eastern SCS showed moderate warming trends due to enhanced vertical mixing and cold-water entrainment (Liu *et al*., 2020). Significant freshening is observed through the SWM, with SSS declines exceeding -1.2% along the southern and eastern coasts, indicating strong freshwater input. During the NEM, localised reductions (~ -1.3%) were observed near the Sabah coast but were less widespread (Figure 6).

Significant reductions in NH_4 all through the SWM (-51.9%) and a corresponding drop in O_2 levels (down to -14.6%), indicate intensified nutrient uptake and deoxygenation. During SWM, NO_3 levels show a moderate to strong increase in central and southern SCS, with percent changes ranging between 5.5% and 65%, peaking notably near 4 °N – 10 °N and 104° E – 114° E (Figure 5). In contrast, during DJF, NO_3 increases are more widespread but relatively lower in magnitude, with values ranging between -9% and 65%, particularly elevated in the Gulf of Thailand (>10 °N).

Next, during SWM, the coastal zones of western and southern SCS show moderate increases in diatom biomass, with values between -15.9% to 42.1% while much of the eastern SCS experienced a more pronounce decrease, especially off the eastern Sabah coast, with reductions ranging between -35.2% and -73.8%. While, during the NEM, most of the central values ranging between -3.2% and -24.1%, some localised patches reaching below -24.1%, especially in offshore and deeper waters. Positive changes, reaching up to ~70% were only observed near the northwestern coastal zone – GoT, indicating localised enhancement during winter.

The projected percent change maps reveal a notable decline in phytoplankton and zooplankton across both seasons. During NEM, phytoplankton exhibited a marked decrease of down to -21.9% along the east coast of Peninsular Malaysia and Sabah while increases of up to +50.9% occurring mainly in the western and northern SCS. Similarly, zooplankton showed widespread reductions, down to -26.6%, particularly around the central southern SCS, with limited positive anomalies near the Sabah coast.

During the SWM, the magnitude of the change was more pronounced. Phytoplankton declined substantially, exceeding -71% along the eastern and southeastern areas of the SCS while localised increases up to +50% were observed off the 1GoT. Zooplankton also experienced a sharper reduction, down to -31.8% in the same region (Figure 6). These results suggest decoupling of lower and upper trophic levels under future conditions, particularly in nutrient-rich upwelling and marginal zones, potentially altering trophodynamic balance and ecosystem productivity.

Increased temperature and reduced salinity, as seen in this projection may result in increased water column stratification, which can suppress vertical nutrient mixing, reduce oxygen replenishment at depth. This leads to lower primary productivity, especially during the SWM, as shown by sharp declines in diatoms, phytoplankton, and zooplankton indicating weakened energy transfer to higher trophic levels (Behrenfeld *et al*., 2006; Bopp *et al*., 2013).

Deoxygenation, with O_2 levels dropping by up to -14.6%, may lead to hypoxic conditions, threatening benthic organisms and sensitive fish species. While some mobile species (e.g., pelagic fish, cephalopods, crustaceans) may migrate to avoid stress, many cannot adapt quickly enough to the environmental condition changes. However, benthic organisms such as molluscs, echinoderms, and sessile invertebrates are far more vulnerable. Extended exposure to low-oxygen conditions may impair their respiration, feeding, and reproductive systems, ultimately leading to population collapse or species redistribution (Vaquer-Sunyer & Duarte, 2008). These changes risk ecosystem disruption, biodiversity loss, and reduced fisheries productivity (Gruber 2011; Breitburg *et al*., 2018).

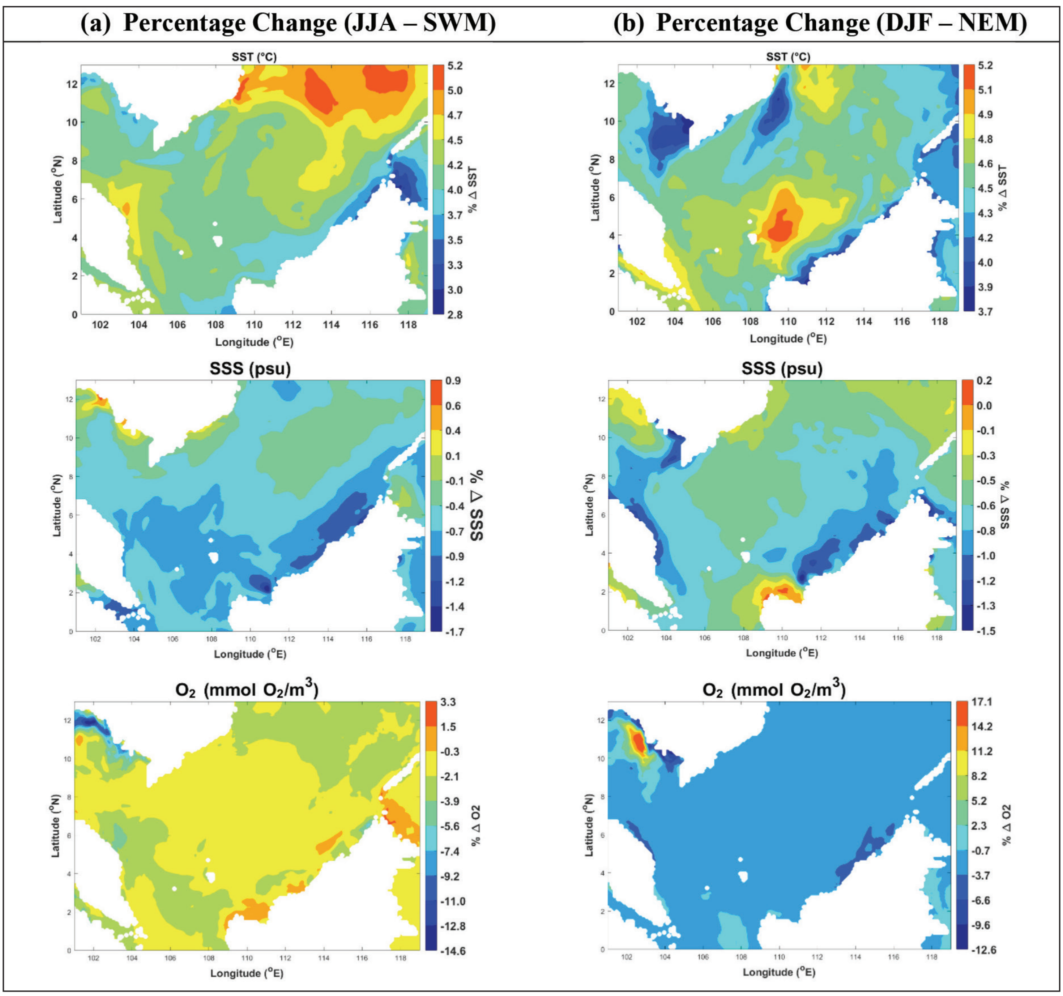

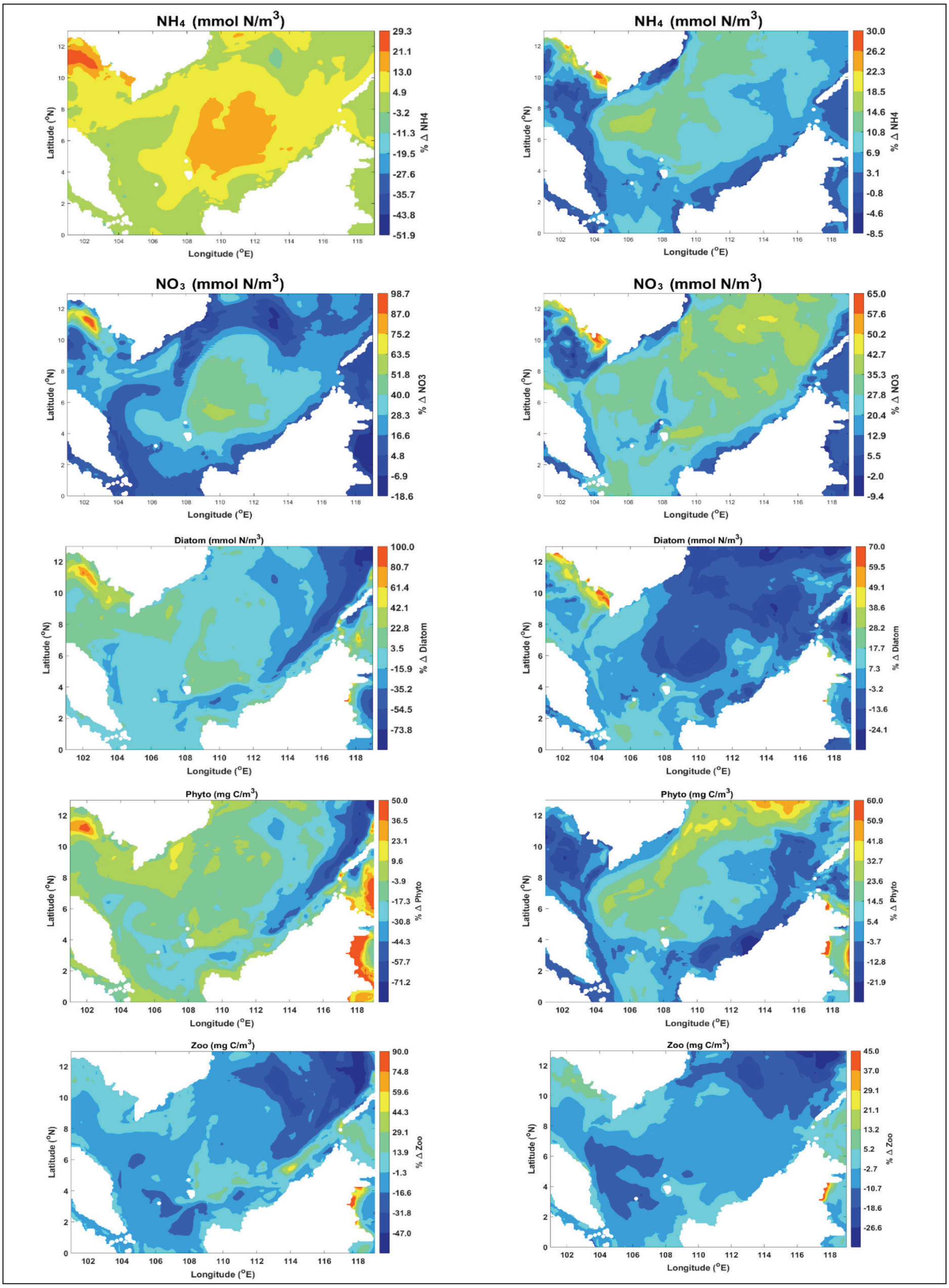

Figure 6: Percentage change of eight surface physical-biogeochemical parameters during (a) JJA represents SWM and (b) DJF represents NEM. Percentage change was calculated by taking the difference between baseline and future decadal values, dividing it by their average, and expressing the result as a percentage (%)

While percentage change in spatial variations of physical-biogeochemical changes across three upwelling zones were discussed earlier, Table 2 summarises the most significant and region-wide projected changes in the SCS region. SST shows a strong warming (~ +5.2%) across both seasons and declines in sea surface salinity (~ -1.5%), which suggest enhanced freshwater input likely driven by increased precipitation and runoff (Capotondi *et al*., 2012). Notable reductions in O_2 (~ -10%), microphytoplankton (~ -19.9%), and microzooplankton (~ -10.7%) all through the NEM indicate a broader trend of deoxygenation and productivity loss, consistent with global projections (Laufkotter *et al*., 2015; Breitburg *et al*., 2018). Nutrient changes (e.g., NH_4 and NO_3) display strong seasonal contrasts, reflecting complex monsoon-driven biogeochemical dynamics in the SCS (Yang *et al*., 2024).

Conclusions

This study, using a single regional-scale model driven by a single global climate model, offers important insights into the potential impacts of climate change across the SCS. Projections under the RCP8.5 climate change scenario indicate intensified surface ocean warming, salinity falling, nutrient shifts, deoxygenation, and productivity loss particularly during the SWM. The projected changes to the mean state and seasonality of physical and biogeochemical ocean conditions pose significant challenges to diverse marine ecosystem. Marine organisms may face heightened stress from simultaneous exposure to multiple stress factors such as warming oceans, deoxygenation, and nutrient loss, underscoring the urgent need for substantial emission reductions.

Table 2: Percentage change in surface physical-biogeochemical parameters in SCS from 1990 to 2060 during SWM and NEM. Values represent the projected percentage change under the RCP8.5 scenario based on NEMO-ERSEM model outputs. Notable trends highlight the most significant seasonal response across parameters

No.	Parameters	Unit	Percentage of Change (%)		Notable Trend
			SWM (JJA)	NEM (DJF)	
1	SST	°C	5.2	5.0	Strong warming in both monsoon seasons
2	SSS	psu	-1.3	-1.5	Salinity decline
3	O_2	mmol O_2/m³	-0.3	-10.0	Significant oxygen depletion during NEM
4	NH_4	mmol N/m³	21.1	-4.6	Large increase during SWM, moderate decline during NEM
5	NO_3	mmol N/m³	-6.9	12.9	Decline in SWM, increase in NEM
6	Diatom nitrogen	mmol N/m³	3.5	-13.6	Slight increase in SWM, strong decline in NEM
7	Microphytoplankton	mg C/m³	-3.9	-19.9	Notable reduction, especially in NEM
8	Microzooplankton	mg C/m³	-1.8	-10.7	General decline, strong during NEM

However, the study does not quantify the uncertainty associated with these projected changes, an essential consideration for informed decision-making. To enhance confidence in future projections, there is a need for additional simulations using a variety of models with different climate sensitivities and alternative global emission scenarios. This would help estimate uncertainty ranges and provide clearer confidence levels for changes in different variables and locations. In a region known for its exceptional marine biodiversity and where millions depend on the sea for their livelihoods, such projections are vital tools for supporting communities in planning and adapting to the impacts of climate change.

Acknowledgements

The authors gratefully acknowledge the support from the Talent and Publications Enhancement Research Grant (TAPE-RG) [TAPERG/2023/UMT/2383] and the Long-Term Research Grant Scheme (LRGS) provided by Ministry of Higher Education (MoHE), Malaysia [LRGS/1/2020/UMT/01/1]. We also extend our sincere appreciation to Dr. Anna Katavouta and Dr. Jeff Polton for freely providing access to the physical and biogeochemical model outputs in used in this study.

Conflict of Interest Statement

The authors declare that they have no conflict of interest.

References

Barange, M., Merino, G., Blanchard, J. L., Scholtens, J., Harle, J., Allison, E. H., Allen, J. I., Holt, J., & Jennings, S. (2014). Impacts of climate change on marine ecosystem production in societies dependent on fisheries. *Nature Climate Change*, *4*, 211–216. https://doi.org/10.1038/nclimate2119

Behrenfeld, M. J., O'Malley, R. T., Siegel, D. A., McClain, C. R., Sarmiento, J. L., Feldman, G. C., Milligan, A. J., Falkowski, P. G., Letelier, R. M., & Boss, E. S. (2006). Climate-driven trends in contemporary ocean productivity. *Nature*, *444*, 752–755. https://doi.org/10.1038/nature05317

Bopp, L., Resplandy, L., Orr, J. C., & Doney, S. C. (2013). Multiple stressors of ocean ecosystems in 21st century: Projections with CMIP5 models. *Biogeosciences*, *10*(10), 6225–6245. https://doi.org/10.5194/bg-10-6225-2013

Brander, K. (2010). Impacts of climate change on fisheries. *Journal of Marine Systems*, *79*, 389–402. https://doi.org/10.1016/j.jmarsys.2008.12.015

Breitburg, D., Levin, L. A., Oschlies, A., Gregoire, M., Chavez, F. P., Conley, D. J., Garçon, V., Gilbert, D., Gutiérrez, D., Isensee, K., Jacinto, G. S., Limburg, K. E., Montes, I., Naqvi, S. W. A., Pitcher, G. C., Rabalais, N. N., Roman, M. R., Rose, K. A., Seibel, B. A., Telszewski, M., Yasuhara, M., & Zhang, J. (2018). Declining oxygen in global ocean and coastal waters. *Science*, *359*, Article 6371. https://doi.org/10.1126/science.aam7240

Butenschön, M., Clark, J., Aldridge, J. N., Allen, J. I., Artioli, Y., Blackford, J., Bruggeman, J., Cazenave, P., Ciavatta, S., Kay, S., Lessin, G., van Leeuwen, S., & Torres, R. (2016). ERSEM 15.06: A generic model for marine biogeochemistry and the ecosystem dynamics of the lower trophic levels. *Geoscientific Model Development*, *8*, 7063–7187. https://doi.org/10.5194/gmd-9-1293-2016

Cai, W., Pan, A., Roemmich, D., Cowan, T., & Guo, X. (2009). Argo profiles a rare occurrence of three consecutive positive Indian Ocean dipole events, 2006–2008. *Geophysical Research Letters*, *36*(8). https://doi.org/10.1029/2008GL037038

Cai, W., Van Rensch, P., Cowan, T., & Hendon, H. H. (2012). An asymmetry in the IOD and ENSO teleconnection pathway and its impact on Australian climate. *Journal of*

Climate, *25*(18). https://doi.org/10.1175/JCLI-D-11-00501.1

Calbet, A., & Saiz, E. (2005). The ciliate-copepod link in marine ecosystems. *Aquatic Microbial Ecology*, *38*, 157–167. https://doi.org/10.3354/ame038157

Capotondi, A., Alexander, M. A., Bond, N. A., Curchitser, E. N., & Scott, J. D. (2012). Enhanced upper ocean stratification with climate change in the CMIP3 models. *Journal of Geophysical Research*, *117*(C4). https://doi.org/10.1029/2011JC007409

Chen, W., Wang, X., & Yang, S. (2023). Response of phytoplankton community structure to environmental changes in the coastal areas of northern China. *Marine Pollution Bulletin*, *195*, Article 115300. https://doi.org/10.1016/j.marpolbul.2023.115300

Chou, C., Neelin, J. D., Chen, C. A., & Tu, J. Y. (2009). Evaluating the "rich-get-richer" mechanism in tropical precipitation change under global warming. *Journal of Climate*, *22*(8), 1982–2005. https://doi.org/10.1175/2008JCLI2471.1

Clark, D., & Lessin, G. (2019). *Model projections of marine environmental variables response to climate change within England's south west marine plan area* (MMO 1169).

Collins, W. J., Bellouin, N., Doutriaux-Boucher, M., Gedney, N., Halloran, P., Hinton, T., Hughes, J., Jones, C. D., Joshi, M., Liddicoat, S., Martin, G., O'Connor, F., Rae, J., Senior, C., Sitch, S., Totterdell, I., Wiltshire, A., & Woodward, S. (2011). Development and evaluation of an Earth-System model – HadGEM2. *Geoscientific Model Development*, *4*(4), 1051–1075. https://doi.org/10.5194/gmd-4-1051-2011

Deser, C., Phillips, A., Bourdette, V., & Teng, H. (2010). Uncertainty in climate change projections: The role of internal variability. *Climate Dynamics*, *38*, 527–546. https://doi.org/10.1007/s00382-010-0977-x

Fang, C., & Wu, L. (2008). The role of ocean dynamics in tropical Pacific SST response to warm climate in a fully coupled GCM. *Geophysical Research Letters*, *35*(8). https://doi.org/10.1029/2007GL033097

Fu, F. X., Tatters, A. O., & Hutchins, D. A. (2012). Global change and the future of harmful algal blooms in the ocean. *Marine Ecology Progress Series*, *470*, 207–233. https://doi.org/10.3354/meps10047

Good, S., Fiedler, E., Mao, C., Martin, M. J., Maycock, A., Reid, R., Roberts-Jones, J., Searle, T., Waters, J., While, J., & Worsfold, M. (2020). The current configuration of the OSTIA system for operational production of foundation sea surface temperature and ice concentration analyses. *Remote Sensing*, *12*(4), Article 720. https://doi.org/10.3390/rs12040720

Gruber, N. (2011). Warming up, turning sour, losing breath: Ocean biogeochemistry under global change. *Philosophical Transactions of the Royal Society A*, *369*(1943), 1980–1996. https://doi.org/10.1098/rsta.2011.0003

Hastenrath, S. (2015). Tropical meteorology and climate: Tropical climates. In North, G. R., Pyle, J. A., & Zhang, F. (Eds.), *Encyclopedia of atmospheric sciences* (2nd ed., Vol. 6).

Hu, J., Kawamura, H., Hong, H., & Qi, Y. (2000). A review on the currents in the South China Sea: Seasonal circulation, South China Sea warm current and Kuroshio intrusion. *Journal of Oceanography*, *56*, 607–624. https://doi.org/10.1023/A:1011117531252

IPCC. (2019). *Climate change 2019: The physical science basis. Contribution of Working Group I to the Fifth Assessment Report of the Intergovernmental Panel on Climate Change*. Cambridge University Press.

Jacobs, Z. L., Yool, A., Jebri, F., Srokosz, M., Gennip, S. V., Kelly, S. J., Roberts, M., Sauer, W., Queirós, A. M., Osuka, K. E., Samoilys, M., Becker, A. E., & Popova, E. (2021). Key climate change stressor of marine ecosystems along the path of the East African coastal current. *Ocean & Coastal Management*, *208*, Article 105527. https://doi.org/10.1016/j.ocecoaman.2021.105627

Katavouta, A., Polton, J. A., Harle, J. D., & Holt, J. T. (2022). Effect of tides on the Indonesian Sea circulation and their role on the volume, heat, and salt transport of the Indonesian Throughflow. *Journal of Geophysical Research: Oceans*, *127*(8). https://doi.org/10.1029/2022JC018524

Kay, S., Avillanosa, A. L., Cheung, V. V., Dao, H. N., Gonzales, B. J., Palla, H. P., Praptiwi, R. A., Queirós, A. M., Sailley, S. F., Sumeldan, J. D. C., Syazwan, W. M., Then, A. Y. H., & Wee, H. B. (2023). Projected effects of climate change on marine ecosystems in southeast Asian seas. *Frontiers in Marine Science*, *10*. https://doi.org/10.3389/fmars.2023.1082170

Knutson, T., Camargo, S. J., Chan, J. C. L., Emmanuel, K., Ho, C. H., Kossin, J., Mohapatra, M., Satoh, M., Sugi, M., Walsh, K., & Wu, L. (2020). Tropical cyclones and climate change assessment: Part II: Projected response to anthropogenic warming. *Bulletin of the American Meteorological Society*, *101*, E303–E322. https://doi.org/10.1175/BAMS-D-18-0194.1

Kok, P. H., Akhir, M. F., & Qiao, F. (2019). Distinctive characteristics of upwelling along the peninsular Malaysia's east coast during 2009/10 and 2015/16 El Niños. *Continental Shelf Research*, *184*, 10–20. https://doi.org/10.1016/j.csr.2019.07.004

Kulk, G., Platt, T., Dingle, J., Jackson, T., Jonsson, B. F., Bouman, H. A., Babin, M., Brewin, R. J. W., Doblin, M., Estrada, M., Figueiras, F. G., Furuya, K., González-Benítez, N., Gudfinnsson, H. G., Gudmundsson, K., Huang, B., Isada, T., Kovač, Z., Lutz, V. A., … Sathyendranath, S. (2020). Primary production, an index of climate change in the ocean: Satellite-based estimates over two decades. *Remote Sensing*, *12*(5). https://doi.org/10.3390/rs12050826

Kwiatkowski, L., Torres, O., Bopp, L., Aumont, O., Chamberlain, M., Christian, J. R., Dunne, J. P., Gehlen, M., Ilyina, T., John, J. G., Lenton, A., Li, H., Lovenduski, N. S., Orr, J. C., Palmieri, J., Santana-Falcón, Y., Schwinger, J., Séférian, R., Stock, C. A., … Ziehn, T. (2020). Twenty-first century ocean warming, acidification, deoxygenation, and upper-ocean nutrient and primary production decline from CMIP6 model projections. *Biogeosciences*, *17*(13), 3439–3470. https://doi.org/10.5194/bg-17-3439-2020

Lam, V. M. Y., Allison, E. H., Bell, J. D., Blythe, J., Cheung, W. W. L., Frölicher, T. L., Gasalla, M. A., & Sumaila, U. R. (2020). Climate change, tropical fisheries and prospects for sustainable development. *Nature Reviews Earth & Environment*, *1*, 440–454. https://doi.org/10.1038/s43017-020-0071-9

Laufkötter, C., Vogt, M., Gruber, N., Aita-Noguchi, M., Aumont, O., Bopp, L., & Völker, C. (2015). Drivers and uncertainties of future global marine primary production in marine ecosystem models. *Biogeosciences*, *12*, 6955–6984. https://doi.org/10.5194/bg-12-6955-2015

Lee, T. C., Knutson, T. R., Kamahori, H., & Ying, M. (2012). Impacts of climate change on tropical cyclones in the Western North Pacific Basin. Part I: Past observations. *Tropical Cyclone Research and Review*, *1*(2), 213–235. https://doi.org/10.6057/2012TCRR02.08

Liu, K. K., Chao, S. Y., Shaw, P. T., Gong, G. C., Chen, C. C., & Tang, T. Y. (2002). Monsoon-forced chlorophyll distribution and primary production in South China Sea: Observations and numerical study. *Deep Sea Research Part I: Oceanographic Research Papers*, *49*(8), 1387–1412. https://doi.org/10.1016/S0967-0637(02)00035-3

Loo, Y. Y., Billa, L., & Singh, A. (2015). Effect of climate change on seasonal monsoon in Asia and its impact on the variability of monsoon rainfall in Southeast Asia. *Geoscience Frontiers*, *6*(6), 817–823. https://doi.org/10.1016/j.gsf.2014.02.009

Lu, Z., Gan, J., Dai, M., Zhao, X. & Hui, C.R. (2020). Nutrient transport and dynamics in South China Sea: A modelling study. *Progress in Oceanography*, *183*, 102308. https://doi.org/10.1016/j.pocean.2020.102308

Luo, J. J., Zhang, R., Behera, S. K., Masumoto, Y., Jin, F. F., Lukas, R., & Yamagata, T. (2010). Interaction between the El Niño and extreme Indian Ocean dipole. *Journal of Climate*, *23*(3). https://doi.org/10.1175/2009JCLI3104.1

Ma, W., Chai, F., Xiu, P., Xue, H., & Tian, J. (2013). Modelling the long-term variability of phytoplankton functional groups and primary productivity in the South China Sea. *Journal of Oceanography*, *69*(5). https://doi.org/10.1007/s10872-013-0190-8

Marshal, W., Roseli, N. H., Amin, R. M., & Akhir, M. F. (2025). Long-term biogeochemical variations in the southern South China Sea and adjacent seas: A model data analysis. *Journal of Sea Research*, *204*, Article 102573. https://doi.org/10.1016/j.seares.2025.102573

Neumann, B., Vafeidis, A. T., Zimmermann, J., & Nicholas, R. J. (2015). Future coastal population growth and exposure to sea-level rise and coastal flooding – A global assessment. *PLOS ONE*, *10*(3). https://doi.org/10.1371/journal.pone.0118571

Ning, X., Chai, F., Xue, H., Cai, Y., Liu, C., & Shi, J. (2004). Physical-biological oceanographic coupling influencing phytoplankton and primary production in the South China Sea. *Journal of Geophysical Research: Atmospheres*, *109*(C10). https://doi.org/10.1029/2004JC002365

Ning, X., Lin, C., Hao, Q., Liu, C., Le, F., & Shi, J. (2009). Long term changes in the ecosystem in the northern South China Sea during 1976–2004. *Biogeosciences*, *6*(10), 2227–2243. https://doi.org/10.5194/bg-6-2227-2009

Nur'utami, M. N., & Hidayat, R. (2016). Influences of IOD and ENSO to Indonesian rainfall variability: Role of atmosphere-ocean interaction in the Indo-Pacific sector. *Procedia Environmental Sciences*, *33*. https://doi.org/10.1016/j.proenv.2016.03.070

Pinsky, M. L., Worm, B., Fogarty, M. J., Sarmiento, J. L., & Levin, S. A. (2013). Marine taxa track local climate velocities. *Science*, *341*(6151), 1239–1242. https://doi.org/10.1126/science.1239352

Roseli, N. H., & Akhir, M. F. (2014). Variations of Southern South China Sea characteristics near Pahang. *Sains Malaysiana*, *43*(9), 1389–1396.

Roseli, N. H., Maisarah, N., Shakila, N., Wahid, A., & Irwan, M. S. (2022). Temperature and salinity characteristics in the southern South China Sea and Strait Malacca. *Universiti Malaysia Terengganu Journal of Undergraduate Research*, *4*(1), 99–116. https://doi.org/10.46754/umtjur.v4i1.264

Roxy, M. K., Modi, A., Murtugudde, R., Valsala, V., Panickal, S., Kumar, S. P., Ravichandran, M., Vichi, M., & Lévy, M. (2015). A reduction in marine primary productivity driven by rapid warming over the tropical Indian Ocean. *Geophysical Research Letters*, *43*(2), 826–833. https://doi.org/10.1002/2015GL066979

Schmidtko, S., Stramma, L., & Visbeck, M. (2017). Decline in global oceanic oxygen content during the past five decades. *Nature*, *542*(7641). https://doi.org/10.1038/nature21399

Schwalm, C. R., Glendon, S., & Duffy, P. B. (2020). RCP8.5 tracks cumulative CO_2 emissions. *Proceedings of the National*

Academy of Sciences, *117*(33), 19656–19657. https://doi.org/10.1073/pnas.2007117117

Siang, H. L., Sulong, S., Shah, M. N., Siang, H. Y., Suratman, S., Jye, M. W., & Idris, M. S. (2021). The impact of human altered geomorphology on the seasonal distribution pattern of water physicochemical and nutrient parameters in Terengganu River estuary Malaysia. *Journal of Sustainability Science and Management*, *17*, 212–235. http://doi.org/10.46754/jssm.2022.4.016

Soumya, M., Vethamony, P., & Tkalich, P. (2015). Inter-annual sea level variability in the Southern South China Sea. *Global and Planetary Change*, *133*, 17–26. https://doi.org/10.1016/j.gloplacha.2015.07.003

Steinacher, M., Joos, F., Frölicher, T. L., Bopp, L., Cadule, P., Cocco, V., Doney, S. C., Gehlen, M., Lindsay, K., Moore, J. K., Schneider, B., & Segschneider, J. (2010). Projected 21st century decrease in marine productivity: A multi-model analysis. *Biogeosciences*, *7*(3), 979–1005. https://doi.org/10.5194/bg-7-979-2010

Stobutzki, I. C., Silvestre, G. T., & Garces, L. R. (2006). Key issues in coastal fisheries in South and Southeast Asia, outcomes of a regional initiative. *Fisheries Research*, *78*(2–3), 109–118. https://doi.org/10.1016/j.fishres.2006.02.002

Sumaila, U. R., Cheung, W. W. L., Lam, V., Pauly, D., & Herrick, S. (2011). Climate change impacts on the biophysics and economics of world fisheries. *Nature Climate Change*, *1*(9), 449–456. https://doi.org/10.1038/nclimate1301

Tan, C. K., Ishizaka, J., Matsumura, S., Yusoff, F. M., & Mohamed, M. I. H. (2006). Seasonal variability of SeaWiFS chlorophyll a in the Malacca Straits in relation to Asian monsoon. *Continental Shelf Research*, *26*(2), 168–178. https://doi.org/10.1016/j.csr.2005.09.008

Tao, Z., Wang, S., Chi, X., Zhang, F., & Sun, S. (2025). Zooplankton community structure and vertical distribution in South China Sea during the summer season. *Marine Pollution Bulletin*, *215*, Article 117857. https://doi.org/10.1016/j.marpolbul.2025.117857

Teh, L. S. L., Cashion, T., Alava Saltos, J. J., Cheung, W. W. L., & Sumaila, U. R. (2019). Status, trends, and the future of fisheries in the East and South China Seas. *Fisheries Centre Research Reports*, *27*(1), 101. https://dx.doi.org/10.14288/1.0379884

Thia-Eng, C., Gorre, I. R., Adrian Ross, S., Bernad, S. R., Gervacio, B., & Corazon-Ebarvia, M. (2000). The Malacca Straits. *Marine Pollution Bulletin*, *41*(1–6), 160–178. https://doi.org/10.1016/S0025-326X(00)00108-9

van Vuuren, D. P., Edmonds, J., Kainuma, M., Riahi, K., Thomson, A., Hibbard, K., Hurtt, G. C., Kram, T., Krey, V., Lamarque, J. F., Masui, T., Meinshausen, M., Nakicenovic, N., Smith, S. J., & Rose, S. K. (2011). The representative concentration pathways: An overview. *Climatic Change*, *109*, 5. https://doi.org/10.1007/s10584-011-0148-z

Vaquer-Sunyer, R., & Duarte, C. M. (2008). Thresholds of hypoxia for marine biodiversity. *Proceedings of the National Academy of Sciences*, *105*(40), 15452–15457. https://doi.org/10.1073/pnas.0803833105

Weatherdon, L. V., Magnan, A. K., Rogers, A. D., Sumaila, U. R., & Cheung, W. W. L. (2016). Observed and projected impacts of climate change on marine fisheries, aquaculture, coastal tourism, and human health: An update. *Frontiers in Marine Science*, *3*. https://doi.org/10.3389/fmars.2016.00048

Yang, J., Lin, X., & Wu, D. (2013). On the dynamics of the seasonal variation in the South China Sea throughflow transport. *Journal of Geophysical Research: Oceans*, *118*(12), 6854–6866. https://doi.org/10.1002/2013JC009367

Yang, S., Chen, D., & Deng, K. (2024). Global effects of climate change in the South China Sea and its surrounding areas. *Ocean–Land–Atmosphere Research*, *3*, Article 0038. https://doi.org/10.34133/olar.0038

Ying, M., Knutson, T. R., Kamahori, H., & Lee, T. C. (2012). Impacts of climate change on tropical cyclones in the Western North Pacific Basin. Part II: Late twenty-first century projections. *Tropical Cyclone Research and Review*, *1*(2), 231–241. https://doi.org/10.6057/2012TCRR02.09

Zhang, S., Jennerjahn, T. C., Chen, F., & Jin, G. (2023). Editorial: Changing biogeochemical and ecological dynamics in South China Sea in times of global change. *Frontiers in Marine Science*, *10*. https://doi.org/10.3389/fmars.2023.1165859

Zhang, Y., Li, J., Xue, J., Zheng, F., Wu, R., Ha, K. J., & Feng, J. (2019). The relative roles of the South China Sea summer monsoon and ENSO in the Indian Ocean dipole development. *Climate Dynamics*, *53*(11). https://doi.org/10.1007/s00382-019-04953-4

Zhu, J., Yang, Y., Wang, H., Gao, J., Liu, C., Wang, P., & Liao, H. (2024). Impact of projected changes in sea surface temperature on ozone pollution in China toward carbon neutrality. *Science of The Total Environment*, *915*, Article 170024. https://doi.org/10.1016/j.scitotenv.2024.170024

Zhu, Y., Sun, J., Wang, Y., Li, S., Xu, T., Wei, Z., & Qu, T. (2019). Overview of the multi-layer circulation in the South China Sea. *Progress in Oceanography*, *175*, 171–182. https://doi.org/10.1016/j.pocean.2019.04.001